GEOPHYSICAL RESEARCH LETTERS, VOL. 35, L08309, doi:10.1029/2008GL033665, 2008

Phase equilibria trigger for explosive volcanic eruptions

Sarah J. Fowler[1] and Frank J. Spera[1]

Received 18 February 2008; revised 20 March 2008; accepted 26 March 2008; published 25 April 2008.

[1] A mechanism for explosive volcanic eruptions based on multicomponent phase equilibria modelling of four explosive volcanic systems is proposed. In each system, either isochoric or isobaric crystallization, where either crystals or crystals and exsolved fluid are chemically fractionated from melt, leads inevitably to near-solidus dynamical instability culminating in violent explosive eruption. Driving this instability is a dramatic increase in the volume fraction of fluid bubbles in the magma exceeding the limit for magma fragmentation. This phenomenon is independent of magma decompression. Country rock may be weak, allowing magma to remain in lithostatic equilibrium with its host rock, or strong, leading to divergence of magma and lithostatic pressure. Bubbles may be retained or expelled during crystallization. Instability is the inevitable outcome of crystallization at shallow levels in the crust for all four systems, regardless of the mechanical state of host country rock. We speculate that this phase equilibria mechanism driving explosive eruptions has general significance. **Citation:** Fowler, S. J., and F. J. Spera (2008), Phase equilibria trigger for explosive volcanic eruptions, *Geophys. Res. Lett.*, *35*, L08309, doi:10.1029/2008GL033665.

1. Introduction

[2] Large-volume explosive eruptions of silicic magma are the most powerful volcanic phenomena, involving withdrawal of hundreds to thousands of cubic kilometres of magma at rates of up to 10^9 kg/s and formation of plumes extending into the stratosphere with attendant climatic effects. Thermodynamic models of multicomponent silicate melts [e.g., *Ghiorso and Sack*, 1995] and fluid dynamical simulations [e.g., *Dobran*, 2001] have brought insight into silicic magma petrogenesis and the dynamics of pre-eruptive magma bodies, volcanic conduits, and volcanic jets. However, the capacity of phase equilibria to determine the ultimate dynamic fate of magma (fragmentation and eruption or stagnation and pluton formation) has not been fully explored. Here we propose a triggering mechanism for explosive eruptions based on the phase equilibria and transport properties of four large-volume (V_E) silicic explosive systems. We investigate phase equilibria in the Otowi ($V_E \sim 400$ km^3) and Tshirege ($V_E \sim 200$ km^3) members of the Bandelier Tuff, the 600 km^3 Bishop Tuff, and the deposits from the calderas (2500, 300, and 1000 km^3) of the Yellowstone volcanic field. These represent the six largest eruptions within North America over the past 2 Ma [*Lowenstern et al.*, 2006]. We compare these rhyolitic systems to the 39.3 ka, 200 km^3 trachytic Campanian Ignimbrite, Italy, the largest explosive eruption in the Mediterranean area in the last 200 kyr [*De Vivo et al.*, 2001; *Fowler et al.*, 2007], to evaluate the general applicability of the proposed trigger mechanism. For each system, we show that crystal fractionation, accomplished either isobarically or isochorically, invariably leads to a volume fraction of fluid bubbles in magma exceeding the critical value for magma fragmentation. This mechanism is independent of magma decompression; it occurs even when the magma pressure increases near the solidus during isochoric solidification.

[3] The phase equilibria calculations are based on the MELTS algorithm [*Ghiorso and Sack*, 1995; *Asimow and Ghiorso*, 1998]. MELTS provides internally consistent phase equilibria solutions based on rigorous thermodynamics by decomposing the evolution of a system into a series of steps subject to appropriate thermodynamic and mass balance constraints. Equilibrium relies upon minimization of a suitable thermodynamic potential of selected independent variables. In this study, crystals precipitating from melt are immediately removed (fractionated) from the system, preventing further reaction. In contrast, fluid bubbles of pure H_2O, the only volatile constituent considered, either (1) remain in chemical potential equilibrium with residual melt or (2) are treated like crystals and are immediately chemically separated from magma. Figure 1 shows a classification of thermodynamic and mass transfer paths associated with crystallization and fluid exsolution during magma evolution. We consider four of the possible eight paths (Figure 1). Specifically, we consider isobaric and isochoric solidification with fractionation of either precipitated crystals and exsolved fluid or fractionation of crystals only. We show that regardless of thermodynamic process or fractionation constraint, each system evolves to a condition whereby the volume fraction of the exsolved supercritical fluid phase (θ) dramatically increases beyond the critical limit for magma fragmentation of $\sim$0.7 [*Papale*, 1999; *Zhang et al.*, 2007]. This eruption trigger mechanism is distinct from the instability associated with magma decompression, which also leads to a rapid increase in θ. Although the idea of volatile exsolution-driven eruption has existed for a long time, our novel contribution is to describe the process by internally consistent multiphase-multicomponent calculations for specific natural systems. The comparison of prediction with observation enables us to test the model quantitatively unlike earlier studies. In addition, we demonstrate the general applicability of this process by testing four volcanic systems and by showing that the eruption trigger is independent of the mechanical properties of the crust.

2. Modelling Isobaric and Isochoric Crystallization

[4] For the systems studied, petrological and geochemical analysis suggests that crystal fractionation is an important

[1]Department of Earth Science, University of California, Santa Barbara, USA.

0094-8276/08/2008GL033665$05.00

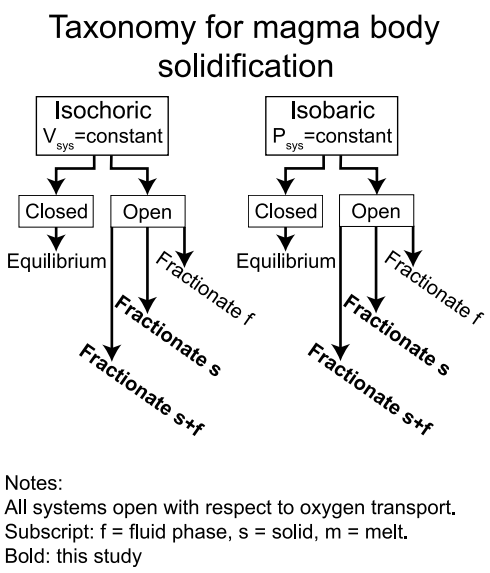

Figure 1. Classification of thermodynamic and mass transfer paths associated with crystallization and fluid exsolution during magma evolution. Bold text indicates the paths that are investigated in this study.

process [*Hildreth et al.*, 1991; *Fowler et al.*, 2007; *Chang et al.*, 2007; *Hildreth and Wilson*, 2007; *Rowe et al.*, 2007]. Although debate exists over the roles of assimilation, partial melting, and remelting [e.g., *Rowe et al.*, 2007; *Bindeman et al.*, 2008], we assume that fractional crystallization is the dominant mechanism of magma evolution and study the implications.

[5] Melt bulk compositions chosen as parental melts used in the calculations are tabulated at ftp://agu.org/apend/. We assume that parental melt containing a fixed amount of dissolved H_2O is emplaced near its liquidus. Temperature is decremented in 10°C steps, with oxygen fugacity set at a buffer (e.g. QFM). We have investigated solidification under isobaric (constant pressure) and isochoric (constant volume) conditions. These conditions are considered limiting cases in natural systems, depending on the mechanical linkage between magma and surroundings. For isobaric solidification ($p_{magma} = p_f = p_m = p_s$; subscripts refer to the fluid, melt and solid phases, respectively), the independent variables include temperature, system bulk composition, oxygen chemical potential, and magma pressure, p_{magma}. Isobaric solidification corresponds to magma solidification in a 'flexible container' that expands (uplift) or contracts (subsidence) to accommodate changes in the system volume ($V_{sys} = V_f + V_m + V_s$). Under isochoric solidification [*Ghiorso and Carmichael*, 1987], volume, rather than magma pressure, is the independent variable; consequently, the magma pressure ($p_{magma} = p_f = p_m = p_s$) evolves during solidification. Isochoric behaviour implies that the country rock forms a 'rigid container'; magma evolution occurs at constant volume. This case is approximated when wallrock deformation is too slow to accommodate volume change due to crystal and fluid bubble formation. Magma is assumed to be in lithostatic equilibrium with host rock at the initiation of solidification. Although natural systems evolve neither at constant volume or pressure it is useful to examine these limits.

[6] We calculated >100 reaction paths based on systematically varying pressure (0.05 to ~0.7 GPa), oxygen fugacity (QFM−3 to QFM+3), and initial water concentration (dry up to H_2O saturation). For each system, we compiled the liquid compositions and mineral types plus compositions of observed eruption products. We then chose those calculations that best correspond to observed compositional data for minerals and liquid lines of descent. We computed phase equilibria for the following cases: (1) isobaric solidification, H_2O fluid bubbles expelled from magma, (2) isobaric solidification, H_2O bubbles retained in magma, (3) isochoric solidification, H_2O bubbles expelled, and (4) isochoric solidification, H_2O bubbles retained (Figures 2, 3, and 4 and auxiliary material[1]).

3. Phase Relations: Isobaric Versus Isochoric Crystallization

[7] The isobaric and isochoric crystallization calculations that best coincide with observational data are characterized by relatively low pressure (0.1−0.3 GPa or 3−8 km depth) and initial dissolved water concentrations of ~3−3.5 wt %, at or near water saturation at the liquidus and initial pressure. Plots comparing predicted major element concentrations and observed data for each system are archived (ftp://agu.org/apend/). The largest discrepancy is for CaO in all cases. The four calculated liquid lines of descent for each system generally overlap, with SiO_2, Al_2O_3, and CaO showing the largest inter-system differences (up to ~2 wt. %) near the solidus. Predicted phenocryst compositions are generally similar, but also reflect minor differences in the modelled reaction paths for each system. In summary, for any system, differences in the liquid line of descent and in the composition of precipitated phenocrysts are relatively small regardless of thermodynamic constraint (isobaric vs. isochoric) and mass balance assumption (fractionate solids only or fractionate solids + fluid bubbles). The largest difference occurs near the solidus for the systems that evolve isochorically because the pressure near the solidus climbs by a factor of two to three over its initial value.

[8] Figure 2 shows a comparison of pressure versus temperature during isochoric solidification, based on fractionation of solids only or solids + H_2O bubbles. The initial pressure for each system is plotted for reference. In all cases, there is a decrease in pressure ($p_{magma} = p_f = p_m = p_s$) until about half of the initial mass of melt has been crystallized. Thereafter, the pressure rises above its initial value for both cases. These results become evident by noting that $\rho_s > \rho_m > \rho_f$, that both fraction solid, f_s, and fraction fluid, f_f, monotonically increase as temperature is lowered and that a significant fluid phase fraction develops only when $f_m < \sim 0.5$. Initially, isochoric crystallization leads to a decrease in the pressure exerted by magma on the wall rock. We speculate that this pressure gradient could lead to episodes of implosive assimilation during the early stages of solidification. In contrast, as temperature approaches the solidus, magma pressure increases above

[1]Auxiliary materials are available in the HTML. doi:10.1029/2008GL033665.

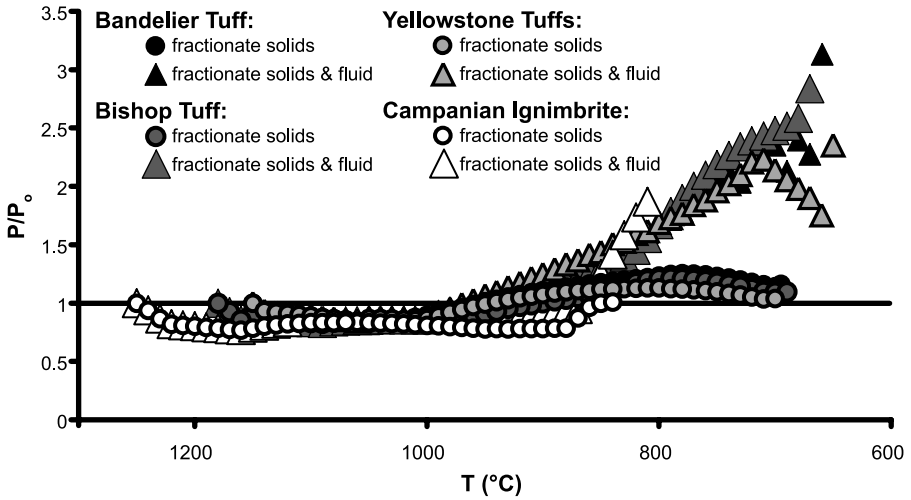

Figure 2. Calculated pressure versus temperature (T) for each system (isochoric calculations only), based on fractionation of solids only and solids + H_2O bubbles.

the initial pressure and attains values sufficient to promote magmafracture and the propagation of magma-filled cracks. If the minimum principal stress, σ_3, is horizontal or sub-horizontal, magma-filled vertical to sub-vertical propagating fractures form provided $p_m > \sigma_3$ + T, where T is the tensile strength of the wall rock, typically ~10 MPa [*Rubin*, 1995]. In summary, pressure differences between magma and country rock during isochoric crystallization can lead to implosive wallrock assimilation in the early stages of solidification, followed by fracture (dike) propagation at later stages. These physical processes can be quantified using the phase equilibria model.

[9] Calculated phase proportions for the four distinct crystallization paths associated with each of the parental compositions share many significant features (Figure 3). In all cases, crystallization begins with olivine followed by clinopyroxene, spinel, and plagioclase. The order of the last two phases depends on the oxygen fugacity; high oxygen fugacity stabilizes early spinel crystallization. At lower temperatures, alkali feldspar (Campanian Ignimbrite and Bishop Tuff) or anorthoclase crystallize. Finally, in all but the Campanian Ignimbrite, quartz saturates very close to the solidus. Very small proportions of other phases also crystallize. For example, apatite crystallizes in all systems, rhombohedral oxide (ilmenite) and orthopyroxene precipitate in the Bandelier, Bishop, and Yellowstone Tuffs, biotite crystallizes in the Campanian Ignimbrite and Bishop Tuff, and fayalite precipitates close to the solidus in the Bandelier Tuff and Yellowstone Tuffs. These predictions are in accord with observations for each system. The important features of Figure 3 are that (1) all systems share remarkably similar crystallization histories regardless of thermodynamic path and (2) eutectic-like crystallization occurs in all systems near the solidus. For the rhyolitic systems, this eutectic-like behaviour is associated with simultaneous feldspar (plagioclase and alkali feldspar) and quartz saturation, whereas for the trachytic Campanian Ignimbrite, plagioclase and alkali feldspar simultaneously saturate. This eutectic-like behaviour leads to a rapid decrease in the melt fraction over a small temperature interval (~few degrees) and drives each system towards magma fragmentation and hence dynamical instability.

4. Magmatic Physical Properties During Isobaric and Isochoric Crystallization

[10] We have examined the physical properties of the systems to relate the phase equilibria to eruption dynamics. In Figure 4, the variation of melt fraction (f_m), dissolved water content, melt density (ρ_m), and volume fraction of fluid in magma (θ) are shown versus temperature. Although in detail each system retains a unique identity subject to the parental composition and the particular thermodynamic and mass balance constraints imposed, a remarkable aspect of Figure 4 is that a universal evolution is apparent.

[11] Melt fraction for all systems decreases monotonically. Plotted in terms of the nondimensional temperature defined as $\bar{T}=\frac{T-T_s}{T_\ell-T_s}$, where T_l and T_s are the liquidus and solidus temperatures, respectively, f_m essentially overlaps for the three rhyolitic systems (Figure 4a). The trachytic Campanian Ignimbrite deviates at f_m >~0.5 and exhibits eutectic-like behaviour [*Fowler et al.*, 2007]. The concentration of dissolved water in the melt is similar for each system, rising from ~3 wt. % to maximum values of ~5–6 wt %. Values are highest for isochoric crystallization because pressure rises (Figure 2) near the solidus and the solubility of water increases with increasing pressure (Figure 4b). In all cases, the melt density decreases by ~10 % as temperature decreases, reflecting the increased dissolved water content of the melt (Figure 4c). Finally, Figure 4d shows the variation of the cumulative volume fraction of fluid (θ) as a function of temperature. For models based on fluid retention, θ surpasses the critical limit for magma fragmentation. For θ greater than the critical limit, a rheological transition occurs in which the topologically connected phase changes from melt to fluid. This rheological transition leads to the viscosity 'collapse' of the magma that we identify as a dynamical eruption trigger generated by the very low density-low viscosity portion of the magma body. For models based on fluid expulsion, a fluid cap would develop at the top of the magma body and could

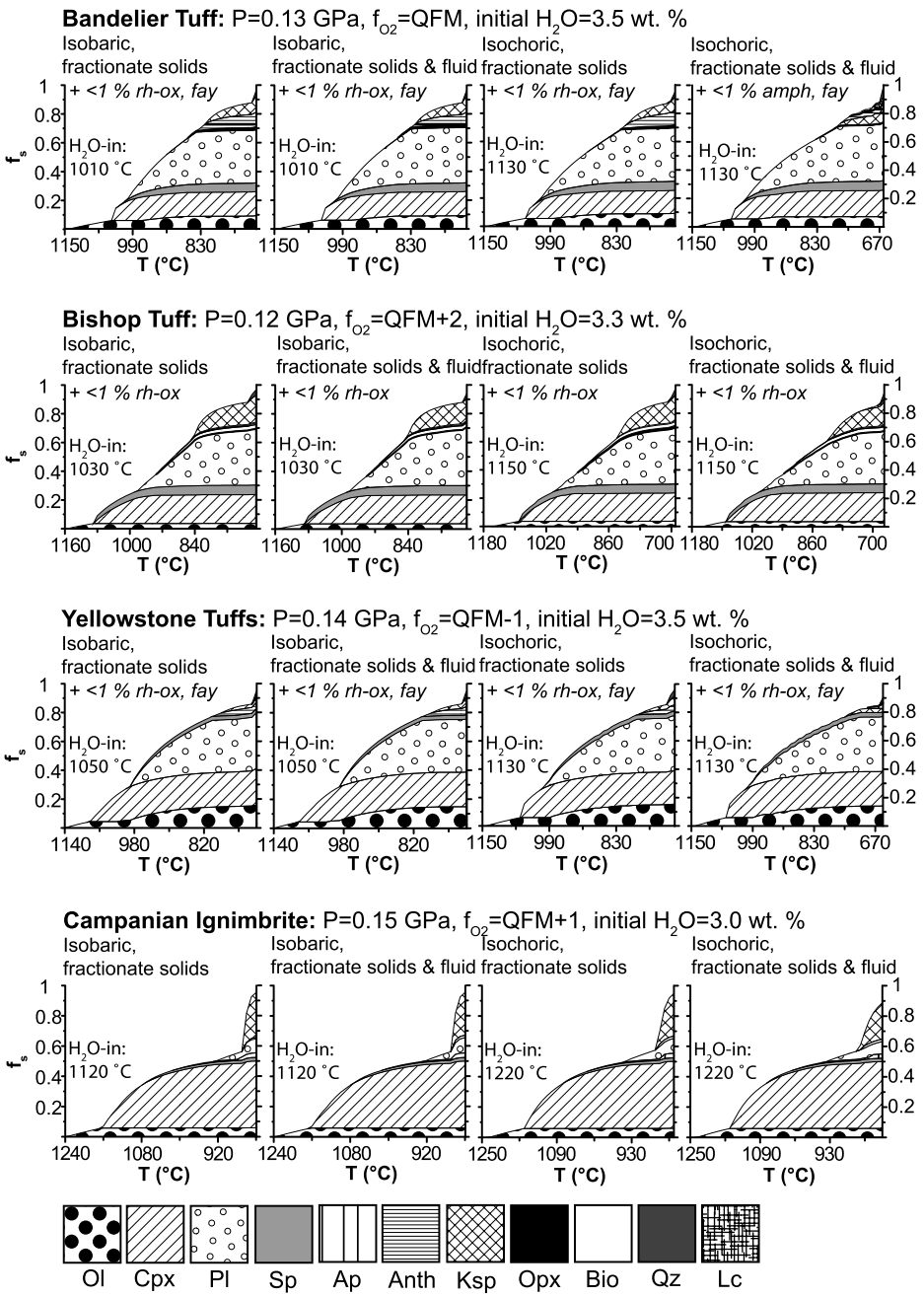

Figure 3. Phase proportions as a function of magma temperature showing the results of crystallization calculations for the four crystallization paths defined in Figure 1 for each volcanic system.

promote roof hydrofracture due to low effective stress values [*Shaw*, 1980].

5. Conclusions

[12] Isobaric and isochoric crystallization with removal of solids and/or fluid represents four magma evolution constraints that bound the conditions under which natural systems evolve. Phase equilibria calculations based on these constraints are broadly similar in terms of major elements, phase compositions, and phase proportions for four large-volume explosive systems, suggesting a general evolution. In all calculations, magma physical properties exhibit variations along the liquid line of descent that culminate near the solidus, setting the stage for explosive giant eruptions. In particular, multiple silicate phase saturation near the solidus leads to abruptly increasing fluid volume fraction in the absence of magma decompression. Depending on the model constraint, eruption can result from fragmentation limit transcendence, increasing melt pressure leading to wallrock failure by crack propagation, or hydrofracture. The pressure increase is greatest when fluid is expelled from melt. For initially H_2O-rich magma hosted at shallow levels by weak or strong country rock, where melt and fluid

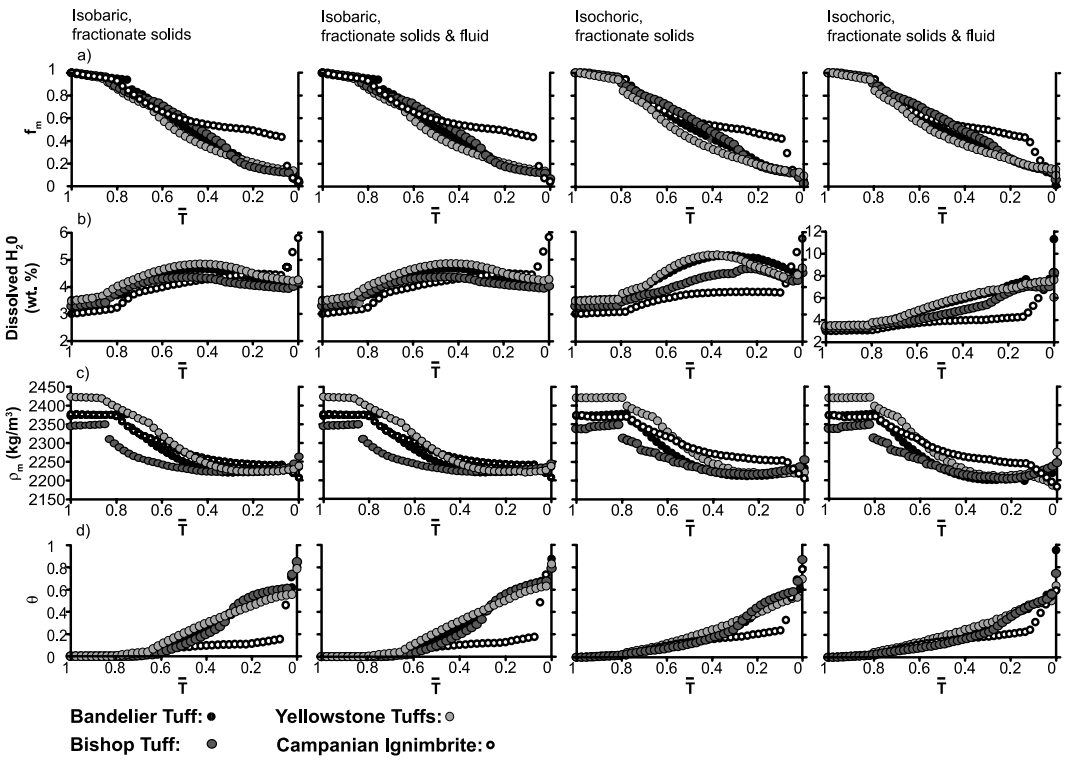

Figure 4. Variation of physical properties along the liquid line of descent versus nondimensional temperature: (a) melt fraction (f_m), (b) dissolved water content of melt, (c) melt density (ρ_m), and (d) volume fraction of exsolved fluid (θ).

are separated or remain in equilibrium, explosive eruption is an inevitable outcome of solidification.

[13] **Acknowledgments.** We thank Mark Ghiorso for critical commentary. Financial Support from the National Science foundation NSF-EAR 0440057 is also gratefully acknowledged.

References

Asimow, P. D., and M. S. Ghiorso (1998), Algorithmic modifications extending MELTS to calculate subsolidus phase relations, *Am. Mineral.*, *83*, 1127–1131.

Bindeman, I. N., B. Fu, N. T. Kita, and J. W. Valley (2008), Origin and evolution of silicic magmatism at Yellowstone based on ion microprobe analysis of isotopically zoned zircons, *J. Petrol.*, *49*, 163–193.

Chang, W.-L., R. B. Smith, C. Wicks, J. M. Farrell, and C. M. Puskas (2007), Accelerated uplift and magmatic intrusion of the Yellowstone Caldera, 2004 to 2006, *Science*, *318*, 952–956.

De Vivo, B., G. Rolandi, P. B. Gans, A. Calvert, W. A. Bohrson, F. J. Spera, and H. E. Belkin (2001), New constraints on the pyroclastic eruptive history of the Campanian volcanic plain (Italy), *Mineral. Petrol.*, *73*, 47–65.

Dobran, F. (2001), *Volcanic Processes: Mechanisms in Material Transport*, 590 pp., Kluwer Acad., New York.

Fowler, S. J., F. J. Spera, W. A. Bohrson, H. E. Belkin, and B. De Vivo (2007), Phase equilibria constraints on the chemical and physical evolution of the Campanian Ignimbrite, *J. Petrol.*, *48*, 459–493.

Ghiorso, M. S., and I. S. E. Carmichael (1987), Modeling magmatic systems: Petrologic applications, in *Thermodynamic Modeling of Geological Materials: Minerals, Fluids and Melts*, *Rev. Mineral.*, vol. 17, edited by I. S. E. Carmichael and H. P. Eugster, pp. 467–499, Mineral. Soc. of Am., Washington, D.C.

Ghiorso, M. S., and R. O. Sack (1995), Chemical mass transfer in magmatic processes. IV. A revised and internally consistent thermodynamic model for the interpolation and extrapolation of liquid-solid equilibria in magmatic systems at elevated temperatures and pressures, *Contrib. Mineral. Petrol.*, *119*, 197–212.

Hildreth, W., and C. J. N. Wilson (2007), Compositional zoning of the Bishop Tuff, *J. Petrol.*, *48*, 951–999.

Hildreth, W., A. N. Halliday, and R. L. Christiansen (1991), Isotopic and chemical evidence concerning the genesis and contamination of basaltic and rhyolitic magma beneath the Yellowstone Plateau volcanic field, *J. Petrol.*, *32*, 63–138.

Lowenstern, J. B., R. B. Smith, and D. P. Hill (2006), Monitoring supervolcanoes: Geophysical and geochemical signals at Yellowstone and other large caldera systems, *Philos. Trans. R. Soc., Ser. A*, *364*, 2055–2072.

Papale, P. (1999), Strain-induced magma fragmentation in explosive eruptions, *Nature*, *397*, 425–428.

Rowe, M. C., J. A. Wolff, J. N. Gardner, F. C. Ramos, R. Teasdale, and C. E. Heikoop (2007), Development of a continental volcanic field: Petrogenesis of pre-caldera intermediate and silicic rocks and origin of the Bandelier magmas, Jemez Mountains (New Mexico, USA), *J. Petrol.*, *48*, 2063–2091.

Rubin, A. M. (1995), Propagation of magma-filled cracks, *Annu. Rev. Earth Planet. Sci.*, *23*, 287–336.

Shaw, H. R. (1980), The fracture mechanism of magma transport from the mantle to the surface, in *Physics of Magmatic Processes*, edited by R. B. Hargraves, pp. 201–264, Princeton Univ. Press, Princeton, N.J.

Zhang, Y., Z. Xu, M. Zhu, and H. Wang (2007), Silicate melt properties and volcanic eruptions, *Rev. Geophys.*, *45*, RG4004, doi:10.1029/2006RG000216.

S. J. Fowler and F. J. Spera, Department of Earth Science, University of California, Santa Barbara, Santa Barbara, CA 93106–9630, USA. (fowler@umail.ucsb.edu)